On the Perturbation of the Intramolecular H-Bond in Diols by Supercritical CO_2: A Theoretical and Spectroscopic Study

Benjamin Renault,[†,‡] Eric Cloutet,[†] Henri Cramail,[†] Thierry Tassaing,*[,‡] and Marcel Besnard[‡]

Laboratoire de Chimie des Polymères Organiques, ENSCPB-CNRS-Université Bordeaux 1 (UMR 5629), 16 Avenue Pey-Berland, 33607 Pessac Cedex, France, and Institut des Sciences Moléculaires, CNRS-Université Bordeaux 1 (UMR 5255), 351 Cours de la Libération, 33405 Talence Cedex, France

Received: November 7, 2006; In Final Form: February 6, 2007

The role played by supercritical carbon dioxide used as a dispersant medium in the synthesis of polyurethane particles has been investigated. High-temperature−high-pressure in situ infrared spectroscopic measurements combined with ab initio calculations were performed to investigate the hydroxyl stretching vibrations of ethylene glycol (EG) and 1,4-butanediol (BD), two monomers commonly used in the field of step growth polymerization. Specific interactions between the diols and CO_2 have been put in evidence. While the structural characteristics of EG and BD are very similar—both diols have a gauche conformation due to an internal H-bond between the two hydroxyl functions—they behave differently in the presence of dense CO_2. In the case of EG, this internal H-bond is broken, allowing the diol and CO_2 to form a complex through the conjunction of a Lewis acid−Lewis base (LA−LB) interaction and a new H-bond. When BD complexes to CO_2, this internal H-bond remains and is even reinforced indirectly by the LA−LB interaction occurring between the two moieties. In both cases, such a complex formation induces a polarization of the hydroxyl groups and consequently an increase of their nucleophilicity.

1. Introduction

Supercritical carbon dioxide ($scCO_2$) has shown great potential as a replacement for conventional aqueous and organic solvents. Indeed, carbon dioxide is a readily available, inexpensive, nontoxic, and nonflammable natural product with easily accessible critical coordinates ($T_c = 31.1$ °C and $P_c = 7.4$ MPa). CO_2 physicochemical properties, such as viscosity and density, can be readily tuned by varying the pressure and the temperature, making it as an attractive medium for polymer synthesis.[1−4] In this field, we recently investigated the synthesis of polyurethanes by polyaddition between either ethylene glycol (EG) or 1,4-butanediol (BD) with tolylene-2,4-diisocyanate (TDI) in the presence of ω-hydroxy poly(dimethylsiloxane) (PDMS−OH).[5,6] In the selected experimental conditions ($T = 60$ °C and $P = 20-40$ MPa), calibrated core−shell polyurethane (PUR) particles with hydrophobic surface properties could be obtained. Additionally, we have found that tin catalyst (DBTDL), generally used in the chemistry of urethanes, was not required in our conditions to obtain high molar mass polymer. This observation prompted us to further investigate the role of $scCO_2$ in polyurethane synthesis. For that purpose, we decided to quantify the specific interactions between CO_2 and the diol, by infrared spectroscopy and ab initio calculations. To our knowledge, diol−CO_2 interactions occurring in this system and modifying the reactivity of the diol toward di-isocyanate comonomer have never been investigated.

Ethylene glycol, a monomer commonly used in step-growth polymerizations for the synthesis of polyesters and polyurethanes, has already been the subject of few experimental and theoretical studies. In particular, it has been shown that EG have numerous conformations due to its three internal rotational degrees of freedom. Several studies using matrix isolation techniques, ab initio molecular orbital methods and density functional theory (DFT) revealed that the lowest energy conformers have a gauche OCCO arrangement stabilized by intramolecular hydrogen bonding.[7−12]

Despite its great interest in polymer chemistry, 1,4-butanediol has not been extensively studied so far. Nevertheless, Traetteberg and Hedberg[13] obtained evidence for internal hydrogen bonding by studying the molecular structure and the conformational equilibrium of the diol using gas-phase electron diffraction. This has been confirmed afterward by Redinha et al.[14] using DFT conformational analysis for all positional BD isomers.

Vibrational spectroscopy combined with ab initio calculations is a powerful tool for probing solute−solvent interactions, since intensities and frequencies associated with vibrational transitions of the solute depend upon the solute−solvent interaction potential.[15−17] As the OH oscillator is known to be very sensitive to molecular interactions, we have used mid-infrared absorption spectroscopy (IR) to probe the OH stretching modes of EG and BD diluted in supercritical CO_2. Such vibrational spectroscopic studies have been previously undertaken on CO_2/monofunctional alcohol mixtures under supercritical conditions. Two types of studies can be distinguished. The first deals with an estimation of the degree of hydrogen bonding of methyl alcohol-*d* [18,19] or ethanol-*d* [20] in supercritical CO_2, whereas the second type of studies is mostly devoted to the nature of the alcohol−CO_2 interaction. Many studies have focused on the latter, and it is now generally accepted that, in the presence of Lewis bases such as water, alcohols, ketones, amines, and amides, CO_2 acts as a Lewis acid favoring the formation of electron donor−acceptor (EDA) complexes.[15,21−25] This terminology has been adopted in the literature as in this kind of complex, the carbon atom of CO_2 points toward the nucleophilic atom of the base

* Corresponding author. E-mail: t.tassaing@ism.u-bordeaux1.fr.
† ENSCPB-CNRS-Université Bordeaux 1 (UMR 5629).
‡ CNRS-Université Bordeaux 1 (UMR 5255).

10.1021/jp0673314 CCC: $37.00
Published on Web 05/03/2007

(oxygen atom in alcohol, water, and ketones and nitrogen atom in amines and amides). However, it is noteworthy that, in such complexes, the charge-transfer interaction contributes only as part of the total stabilization energy and that electrostatic and polarization forces can make comparable and even higher contributions to the energy.[26,27] The existence of such EDA complex formation between alcohols and CO_2 has been put in evidence by both spectroscopic[17,18] and ab initio studies of alcohol−CO_2 systems.[25,28,29]

The purpose of this paper is to analyze and quantify the intermolecular interactions between the two diols described above and CO_2 by means of infrared spectroscopy and ab initio calculations. In this manner, the effect of CO_2 as a dispersant medium onto the diols' reactivity toward isocyanate functions can be better considered.

2. Experimental Details

The measurements were performed on a Biorad interferometer (type FTS-60A) equipped with a globar source, a Ge/KBr beam splitter, and a DTGS detector. Single-beam spectra recorded in the spectral range of 400−6000 cm^{-1} with a 2 cm^{-1} resolution were obtained by Fourier transformation of 50 accumulated interferograms. We used a titanium cell, equipped with four cylindrical windows, two silicium windows for the infrared absorption measurements with a path length of 25 mm, and two sapphire windows for direct observation of the solution. Visual observation ensured that no demixing phenomena occurred in the mixtures which were constantly homogenized during the experiment using a magnetically driven stirrer. The sealing was obtained using the unsupported area principle. The windows were positioned on the flat surface of the titanium plug. A 100 μm Kapton foil placed between the window and the plug compensated for any imperfections between the two surfaces. Flat Teflon seals insured the sealing between the plug and the cell body. Heating was achieved by four cartridge heaters distributed throughout the body of the cell in which two thermocouples were placed. The first one located close to one cartridge is used for the temperature regulation and the second was kept close to the sample area in order to measure the temperature of the sample with an accuracy of about $\Delta T \sim \pm 0.5$ °C. The cell was connected via a stainless steel capillary to a hydraulic pressurizing system which allows the pressure to be raised up to 50 MPa with an absolute uncertainty of ±0.1 MPa and a relative error of ±0.3%. The stabilization of the operating conditions was controlled by recording consecutive spectra. The cell was filled with ethylene glycol-d_2 or 1,4-butanediol-d_{10} ($DOCH_2CH_2OD$ and $DO(CD_2)_4OD$, respectively (Aldrich products, 98% purity)) and heated to the required temperature. CO_2, Ar, or Xe (from the Air Liquide Co.) was then added to the desired pressure.

3. Computational Details

Ab initio and DFT calculations have been carried out using the Gaussian 2003 program suite.[30] Preliminary geometry optimizations were carried out at the Hartree−Fock (HF) level using 6-31G** basis sets. Calculations of geometry, energies, and vibrational frequencies reported in this paper were performed at the second-order Moller−Plesset (MP2) level to include the effects of electron correlation.[31] The geometry optimization calculations have been achieved using the augmented correlation-consistent polarized valence double basis sets (aug-cc-VDZ) proposed by Dunning and co-workers.[32−35] Geometry computation was not subjected to a particular symmetry constraint, excepted for isolated CO_2 ($D_{\infty h}$ symmetry).

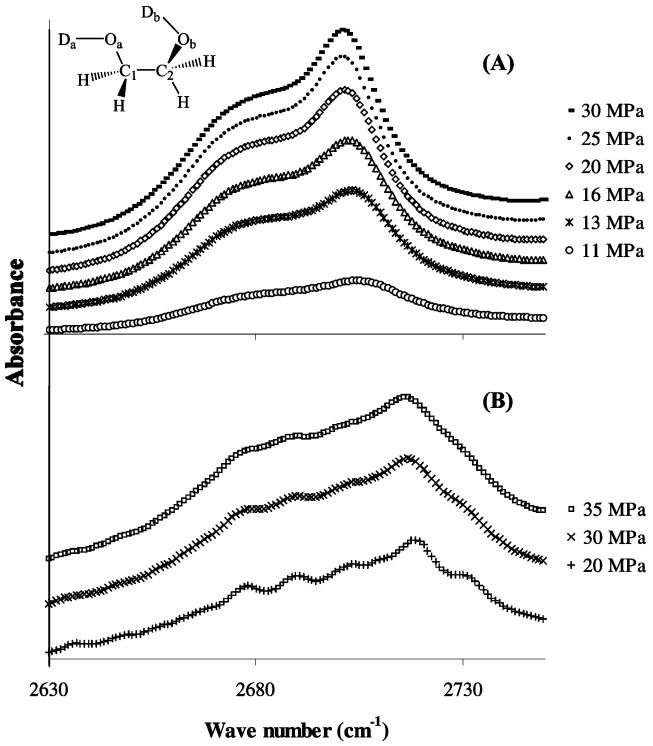

Figure 1. IR spectra of OD stretching modes of EG-d_2 in CO_2 (A) and in Ar (B) at different pressures and constant temperature (60 °C).

The initial configuration used for EG and BD was the lowest energy conformer previously reported by several authors who investigated the conformational properties of these two diols using ab initio and DFT.[7,11,36] Stabilization energy of the diol−CO_2 complex investigated in this paper was calculated using the "supermolecule" method as the difference in energy between each complex and the sum of the isolated monomers. The basis set superposition errors (BSSE) were calculated using the full counterpoise method of Boys and Bernardi.[37] For the equilibrium structure of the diol−$(CO_2)_2$ trimer, the interaction energy calculations explicitly include the irreducible three-body interaction contribution to the total interaction energy according to the site−site function counterpoise scheme.[38,39] Finally, vibrational analyses were carried out within the standard Wilson FG matrix formalism from the appropriate optimized structures of the complex and their corresponding individual moieties at the MP2/aug-cc-VDZ level of calculations.[40] Calculations have been performed on the hydroxyl stretching vibrations of the hydrogenated and deuterated diols, and the calculated frequency values have been corrected using standard scaling factors available from literature[41,42] to allow a comparison with the experimental ones (B3LYP/6-31+G**, 0,9632; MP2/6-31+G*, 0,9398; MP2/aug-cc-pVDZ, 0,95). Molden was used to display the optimized geometry and the vibrational modes of the isolated moieties and the complex.[43]

4. Results and Discussion

4.1. Infrared Spectra of EG Diluted in Ar and CO_2. The IR spectra in the OD stretching region of EG-d_2 diluted in CO_2 (10^{-2} mol·L^{-1}), measured at a constant temperature (T = 60 °C) as a function of pressure (from 11 to 30 MPa), are displayed in Figure 1A. The spectrum at 11 MPa is low because all of the solute is not dissolved at this pressure. We have used hydroxy-deuterated EG instead of fully hydrogenated EG because the strong absorption of combination bands of CO_2 precludes observation of the OH stretching vibration in the

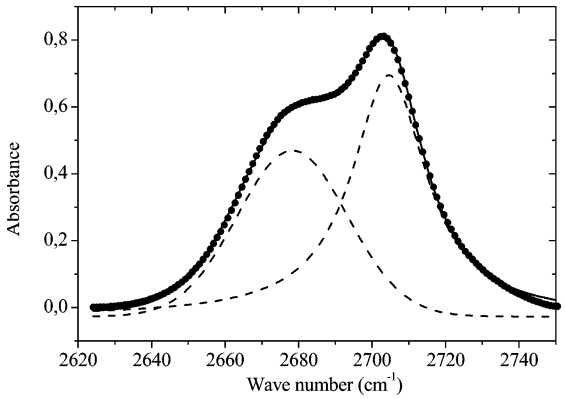

Figure 2. Decomposition of the OD stretching mode for EG-d_2 in CO_2: Experimental spectrum at $T = 60$ °C and $P = 30$ MPa (dots), decomposition of the experimental spectrum (dashed line), and sum of the decomposition of the experimental spectrum (solid line).

spectral range between 3000 and 4000 cm^{-1}. Whatever the pressure is, the infrared spectra display a broad profile exhibiting a doublet structure. After decomposition of the latter, we assigned a well-defined peak centered at 2704 cm^{-1} and a shoulder at about 2678 cm^{-1} (Figure 2). The best fit was achieved using one Lorentzian profile (O_a-D_a stretching mode) and one Gaussian profile (O_b-D_b stretching mode). Both bands are red-shifted with increasing pressure from 11 to 30 MPa. On the basis of previous experimental and theoretical studies,[7−12] these two bands may be assigned to the O_a-D_a and O_b-D_b stretching modes, respectively (see insert Figure 1A). The former is observed at higher frequencies than the latter due to an intramolecular hydrogen bond existing between the D_b and O_a atoms. The absence of any broad spectral feature in the frequency range 2500−2650 cm^{-1} ensures there are no EG hydrogen bonded aggregates. Therefore, in these dilute solutions, EG molecules are under monomeric form and can only interact with surrounding CO_2 molecules.

To put in evidence the spectral signature of existing specific interactions between EG and CO_2, these results have been compared with those obtained for EG-d_2 diluted in supercritical argon ($\approx 10^{-3}$ mol·L^{-1}) under comparable density conditions, the latter being considered as a non-interactive solvent. In particular, scAr and $scCO_2$ have equivalent densities (11.96 mol·L^{-1}) for pressures of 35 and 13 MPa, respectively. The infrared spectra of EG in scAr measured at constant temperature ($T = 60$ °C) and increasing pressure (from 20 to 35 MPa) are reported in Figure 1B. At low pressure (20 MPa), the spectra display a broad band extending over a hundred wave numbers resulting from the overlap of several components roughly spaced by about 10 cm^{-1}. The assignment of the spectral features observed at low pressure is not straightforward. However, this observation and the others as well can be rationalized by considering two facts: (i) the existence of residual vibrational−rotational wings which may be still present but not completely smeared out by collision with the perturbing solvent molecules[17,44,45] and (ii) the EG conformer distribution in the gas phase. As pointed out by Howard et al.,[46] the population of the most stable conformer amounts to about 60%, leaving the possibility to hydroxyl stretching vibrations of less stable conformers (at least two types of species) to be spectrally active.

Disentangling these effects is rather challenging. However, as the pressure increases, the more stable isomer is favored and the solvent collisional frequency increased, thus leading to a simplification of the spectra into a broad profile centered at 2718 cm^{-1} having mostly a distinct shoulder at about 2685 cm^{-1} (Figure 1B). Although the infrared spectra of EG in $scCO_2$ display a comparable doublet structure as that observed in scAr, the gap between the two components, calculated after decomposition of the profile as mentioned above, is significantly reduced, leading to an apparent narrower profile. In particular, the O_a-D_a hydroxyl band appears to be significantly shifted to lower frequency from 2718 (in scAr) to 2704 cm^{-1} (in $scCO_2$). This observation is consistent with a LA−LB interaction between CO_2 and the O_a-D_a hydroxyl group as reported for monoalcohols in spectroscopic[17,18] and ab initio[25,28,29] studies of alcohol−CO_2 systems. More noteworthy are the shift and the narrowing of the band associated with the O_b-D_b hydroxyl group when it is diluted in $scCO_2$ as obtained from the band profile decomposition. Although a band center shift comparable to that observed for the O_a-D_a group may be expected, it is found that the band is only red-shifted from 2685 to 2678 cm^{-1} and significantly narrows from 44 to 35 cm^{-1}. Thus, the frequency gap between the band centers associated with the two hydroxyl groups varies from 33 to 26 cm^{-1} when EG is diluted in Ar and CO_2, respectively. Clearly, this finding reveals a relevant distinction in the way carbon dioxide interacts with both hydroxyl groups.

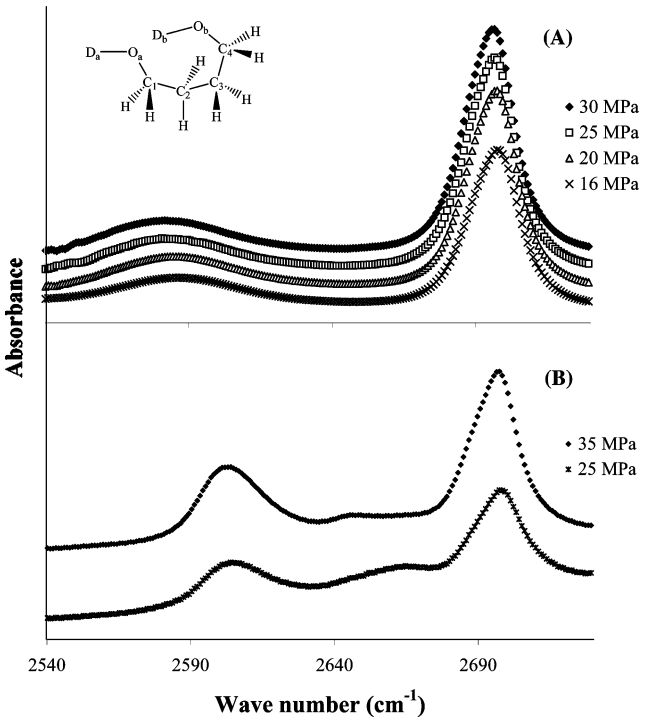

Figure 3. IR spectra of OD stretching modes of BD-d_{10} in CO_2 (A) and in Xe (B) at different pressures and constant temperature (60 °C).

4.2. Infrared Spectra of BD Diluted in Xe and CO_2. The IR spectra in the OD stretching region of BD-d_{10} highly diluted (10^{-2} mol·L^{-1}) in $scCO_2$ have been collected at 60 °C as a function of pressure (Figure 3A). Under these conditions, all the spectra exhibit two absorption bands. The first one, centered at 2696 cm^{-1}, corresponds to the O_a-D_a hydroxyl group, whereas the second centered at 2581 cm^{-1}, is assigned to the O_b-D_b hydroxyl group involved in the intramolecular H-bond occurring between the two alcohol functions.[13,14] As the pressure increases from 16 to 30 MPa, a red shift of the two bands is observed. Because deuterated BD is insoluble in scAr at 60 °C in the pressure range investigated, we have used scXe as a non-interactive solvent to dilute BD in order to characterize the specific interactions between the diol and CO_2. We note that scXe and $scCO_2$ have equivalent densities (16.0 mol·L^{-1}) for pressures of 35 and 19 MPa, respectively. The infrared spectra of BD diluted in scXe at 60 °C mostly display two main

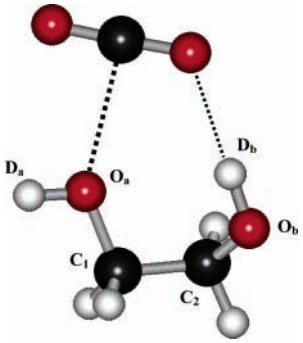

Figure 4. Optimized structure (MP2/aug-cc-pVDZ level) of the EG−CO_2 complex.

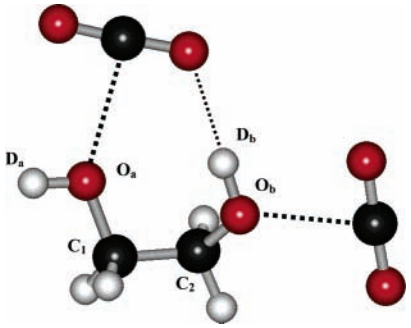

Figure 5. Optimized structure (MP2/aug-cc-pVDZ level) of the EG−$(CO_2)_2$ complex.

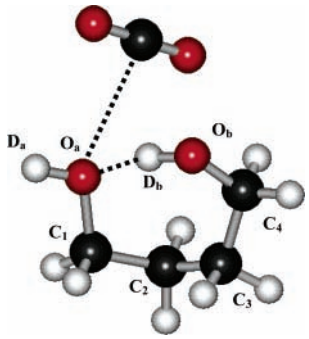

Figure 6. Optimized structure (MP2/aug-cc-pVDZ level) of the BD−CO_2 complex.

absorption bands centered at 2698 and 2604 cm^{-1} (Figure 3B), which are not shifted as the pressure increases from 25 to 35 MPa. In addition, we notice the presence of a broad and faint feature, centered at about 2660 cm^{-1}, between these two bands. As for EG diluted in scAr, the two main peaks can be assigned to a spectral transition belonging to the more stable conformer, leaving the faint spectral feature as due to possible coexistent non-energetically favored conformers (compare Figures 1B and 3B). The main finding is that the infrared spectra of BD in $scCO_2$ display a structure comparable to that observed in scXe, but as clearly seen the relevant difference is in the existing frequency gap between the two bands which is significantly increased in CO_2. Indeed, the O_a-D_a hydroxyl band appears to be weakly shifted to lower frequency from 2698 (in scXe) to 2696 cm^{-1} (in $scCO_2$), while the O_b-D_b hydroxyl group band broadens and shifts significantly from 2604 to 2581 cm^{-1} when it is diluted in $scCO_2$. Thus, the frequency gap between the band centers associated with the two hydroxyl groups varies from 94 to 115 cm^{-1} when BD is diluted in Xe and CO_2, respectively.

4.3. Analysis of the Diols-CO_2 Interactions from ab Initio Calculations. *4.3.1. Structural and Energetic Considerations.* We performed ab initio calculations in order to investigate the origin of molecular interactions responsible for these characteristic spectral shifts. For this purpose, the initial configurations used for each of the diols were taken as the lowest energy conformers previously reported.[7−14] In the case of EG, these studies revealed that the most stable conformer involves a gauche OCCO arrangement stabilized by an intramolecular hydrogen bond between the O_a and D_b atoms, thus forming a strained ringlike molecule. The geometry of the isolated EG−CO_2 pair, fully optimized at the second-order Moller−Plesset perturbation theory (MP2) using Dunning's aug-cc-pVDZ basis set, is displayed in Figure 4. In addition to a LA−LB interaction between the carbon atom of CO_2 and the oxygen atom of the O_a-D_a hydroxyl group pointed out, the optimized geometry clearly shows the existence of an O−D···O interaction between the D_b hydroxyl proton of the EG moiety and one of the oxygen atoms of CO_2. This interaction can be classified as a weak hydrogen bond as it has been found for example in the HF−CO_2 dimer[47] and in the water−CO_2 dimer.[38,48] This additional weak H-bond acts cooperatively with the LA−LB interaction to stabilize the dimer. The calculated binding energy of the complex is −3.46 kcal/mol, including both LA−LB and H-bond interactions. We may compare the interaction energy of the EG−CO_2 pair with that obtained for the ethanol−CO_2 dimer at the same level of calculation. An interaction energy of −2.96 kcal/mol has been found in the latter system for which only the LA−LB interaction takes place.[17] Therefore, we can estimate the contribution due to the cooperative H-bond to be about −0.5 kcal/mol. In this configuration, the ringlike conformation of EG is increased from a five-membered ring ($D_b-O_b-C_2-C_1-O_a$) to a seven-membered ringlike structure including the carbon and an oxygen atom of CO_2. Consequently, the ring strain existing in EG monomer is released when D_b binds the oxygen atom of CO_2. This can be clearly seen in Table 1 as the O_a-D_b distance increases by 221 mÅ on going from EG monomer to EG−CO_2 dimer. As a result, although O−D bonds undergo a lengthening in conventional O−D···O hydrogen bonding, our calculations for the EG−CO_2 complex predict that the hydroxyl O_b-D_b bond shortens by 0.86 mÅ.[23,49] At the same time, the O_a-D_a bond is elongated by 0.82 mÅ due to the LA−LB interaction. Finally, we found that EG in the dimer keeps the same gauche conformation than that of the monomer even if some small deviations of the dihedral angles are observed (Table 1).

To provide a better insight into mechanisms that should take place in dense supercritical CO_2, the geometry optimization of an isolated EG−$(CO_2)_2$ trimer was also carried out at the same level of calculation. The geometry of the EG−$(CO_2)_2$ trimer is displayed in Figure 5. In this configuration, we observe the reminiscent structure of the dimer reported above with the second neighboring CO_2 molecule interacting with the O_b atom of EG through a LA−LB interaction. The calculated binding energy of the complex is −6.28 kcal/mol, including both LA−LB and H-bond interactions. Although the EG−CO_2 complex seems to be only weakly affected by the presence of a second CO_2 molecule, we can observe some small variations in the structural parameters. In particular, it appears clearly from Table 1 that the O_a-D_b distance decreases on going from EG−CO_2 dimer to EG−$(CO_2)_2$ trimer with a concomitant increase by 0.58 mÅ of the O_b-D_b bond. Therefore, the intramolecular structure of EG in the trimer is more EG monomer-like than that in the dimer (except for the O_a-D_a distance). This apparent antagonist effect on the EG molecule might be directly related to the polarization effect induced on the O_b atom by the second CO_2 molecule and a new charge distribution on the EG molecule (see below). Finally, we found, as for the EG−CO_2 dimer, that

TABLE 1: Calculated Relevant Atomic Distances and Dihedral Angles for EG Monomer, EG−CO_2 Dimer, and EG−$(CO_2)_2$ Trimer

	distance (Å)			dihedral angle (deg)		
	O_a-D_a	O_b-D_b	O_a-D_b	$D_aO_aC_1C_2$	$O_aC_1C_2O_b$	$C_1C_2O_bD_b$
EG	0.965 84	0.969 69	2.349 59	−168.588	62.194	−52.007
EG CO_2	0.966 66	0.968 83	2.571 35	−177.609	66.168	−66.425
EG $(CO_2)_2$	0.966 78	0.969 41	2.554 56	−177.949	64.864	−66.811

TABLE 2: Calculated Relevant Atomic Distances and Dihedral Angles for BD Monomer, BD−CO_2 Dimer, and BD−$(CO_2)_2$ Trimer

	distance (Å)			dihedral angle (deg)				
	O_a-D_a	O_b-D_b	O_a-D_b	$D_aO_aC_1C_2$	$O_aC_1C_2C_3$	$C_1C_2C_3C_4$	$C_2C_3C_4O_b$	$C_3C_4O_bD_b$
BD	0.967 53	0.974 66	1.845 64	176.939	76.473	−68.689	74.439	−65.762
BD−CO_2	0.968 12	0.975 14	1.810 52	−177.134	74.023	−76.300	74.611	−52.455
BD−$(CO_2)_2$	0.968 56	0.978 44	1.765 05	−167.616	75.457	−79.128	70.659	−49.105

EG in the trimer keeps the same gauche conformation than that of the monomer even if some small deviations of the dihedral angles are observed (Table 1).

In the case of BD, the initial configuration used for the geometric optimization of a BD−CO_2 dimer is the g′GG′Gt conformation known to be the most stable one due to an intramolecular hydrogen bond between the O_a and D_b atoms.[13,14] The geometry of the fully optimized isolated BD−CO_2 pair (Figure 6) exhibits a LA−LB interaction between CO_2 and the O_a-D_a hydroxyl group in good agreement with the IR spectra described above. The calculated binding energy of the complex is −3.25 kcal/mol. It is noteworthy that this stabilization energy is lower than that reported above for the EG−CO_2 dimer. This difference might be assigned to the cooperative H-bond existing in the EG−CO_2 complex, which does not take place in the BD−CO_2 dimer. Indeed, the intramolecular H-bond existing in BD monomer is not directly perturbed by the presence of the CO_2 molecule. In other words, this intramolecular H-bond is not broken to form an intermolecular H-bond with CO_2 as mentioned above in the case of EG. However, it is clearly seen from Table 2 that the O_a-D_b distance decreases by 35 mÅ on going from BD monomer to BD−CO_2 dimer. This means that the intramolecular H-bond existing in BD monomer is strengthened indirectly by the LA−LB interaction occurring between BD and CO_2. As a result, both O_b-D_b and O_a-D_a bonds are elongated respectively by 0.48 and 0.59 mÅ (Table 2).

The geometry of the isolated BD−$(CO_2)_2$ trimer has been fully optimized using the same level of calculation (Figure 7). In this configuration, we observe the reminiscent structure of the dimer reported above with the second neighboring CO_2 molecule interacting with the O_b atom of BD through a second LA−LB interaction. The calculated binding energy of the complex is −7.37 kcal/mol. This second CO_2 neighboring molecule acts cooperatively with the first CO_2 molecule in the stabilization of the complex. In particular, the intramolecular structure of BD resulting from the dimer formation with one CO_2 molecule is modified in the same way when the complexation with a second CO_2 molecule occurs. Indeed, the O_a-D_b distance still decreases by 45 mÅ on going from the BD−CO_2 dimer to the BD−$(CO_2)_2$ trimer (Table 2). This means that the intramolecular H-bond existing in BD monomer is still strengthened by the second LA−LB interaction. Concomitantly, both O_b-D_b and O_a-D_a bonds are still elongated respectively by 3.3 and 0.44 mÅ.

4.3.2. Vibrational Spectra. EG−CO_2 Complex**.** The calculated harmonic infrared frequencies of EG and its complexes with CO_2 are reported in Figure 8 for the OD stretching region and compared with the experimental infrared spectra of deuterated EG in scAr and CO_2. The calculated frequencies have been scaled using factors available from literature.[41,42] Considering the EG monomer, it appears clearly from this comparison that the two peaks experimentally observed at 2714 and 2674 cm^{-1} can be unambiguously assigned to the O_a-D_a and O_b-D_b stretching modes, respectively. The latter is situated at lower frequency because of the intramolecular hydrogen bond existing in EG monomer. Upon the EG−CO_2 complex formation, we can observe a red shift of 10 cm^{-1} of the O_a-D_a stretching frequency from 2714 to 2704 cm^{-1} due to the LA−LB interaction. However, we observe a blue shift of 9 cm^{-1} of the O_b-D_b stretching frequency from 2674 to 2683 cm^{-1} which can be related to the existence of the $O_b-D_b\cdots O$ interaction between the EG moiety and one of the oxygen atoms of CO_2. Although conventional H-bonds lead to a red shift of the OH frequency, the blue shift observed here for the O_b-D_b stretching frequency is directly related to the shortening of this bond as predicted by our previous calculations on the EG−CO_2 complex (see above). Upon the complex formation of EG with a second CO_2 molecule, we observe that the value of the O_a-D_a stretching frequency is almost unchanged, whereas the O_b-D_b stretching frequency is now red-shifted from 2683 to 2674 cm^{-1} due to the LA−LB interaction occurring between EG and the second CO_2 molecule. Therefore, it appears from Figure 8 that the blue shift (9 cm^{-1}) of the O_b-D_b stretching frequency when EG is complexed with a single CO_2 molecule is almost cancelled by the red shit due to the interaction of the O_b atom with a second CO_2 molecule. This competition explains why although CO_2 is a more interacting solvent than scAr, the O_b-D_b stretching frequencies are not extremely different in both solvents, whereas clearly the vibrational frequency of the O_a-D_a in scCO_2 is observed at much lower frequency than in scAr.

To confirm this conclusion, we performed ab initio calculations using different basis sets (i.e., MP2/6-31+G*, MP2/aug-cc-pVDZ) and DFT calculations using the B3LYP method with the 6-31+G** basis set (Figure 9). The same general trends are observed whatever the basis set used. The O_b-D_b stretching frequency is first blue-shifted when EG is complexed with a single CO_2 molecule and further red-shifted upon complexation as the dimer interacts with a new CO_2 molecule. It is noteworthy that the O_a-D_a stretching frequency remains almost unaffected under this additional complexation. Finally, we must emphasize that the ab initio vibrational spectra calculated at the highest level (MP2/aug-cc-pVDZ) of approximation are in better quantitative agreement with experimental spectra. This is apparent from the scaled frequencies reported for the EG

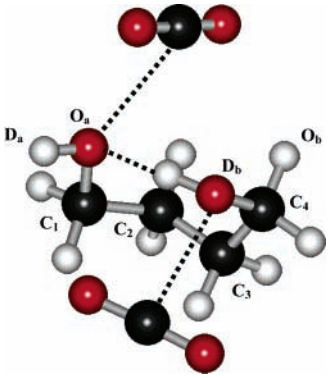

Figure 7. Optimized structure (MP2/aug-cc-pVDZ level) of the BD−$(CO_2)_2$ complex.

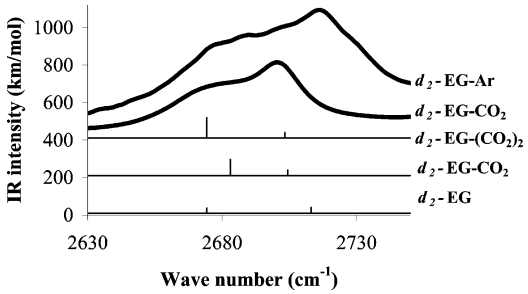

Figure 8. Comparison of the calculated harmonic stretching mode frequencies of EG-d_2 calculated at the MP2/aug-cc-pVDZ computational level (vertical stick) with the experimental IR spectra.

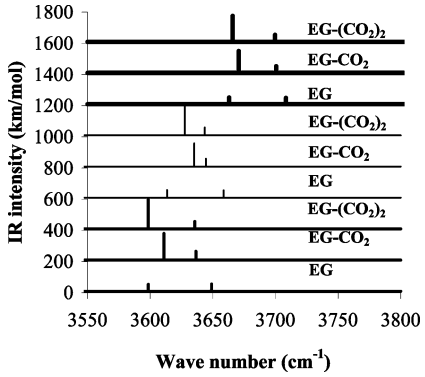

Figure 9. Calculated harmonic O−D stretching frequencies of EG, the EG−CO_2 dimer, and the EG−$(CO_2)_2$ trimer. IR spectra are represented by vertical sticks (from top to bottom B3LYP/6-31+G**, MP2/6-31+G*, MP2/aug-cc-pVDZ, and level of calculation, respectively).

monomer and the $(EG-CO_2)_2$ trimer, which match the experimental infrared spectra of EG in scAr and CO_2, respectively (Figure 8). Clearly, structural investigations of 1:2 complexes provide better insights into mechanisms which take place in dense supercritical CO_2.

BD−CO_2 Complex. The calculated harmonic infrared frequencies of BD-d_{10} monomer and its complexes with CO_2 are reported in Figure 10 for the OD stretching region and compared with the experimental infrared spectra of EG-d_2 in scXe and CO_2. The calculated spectrum of BD monomer in the OD stretching region displays two peaks observed at 2696 and 2585 cm^{-1} which are assigned to the O_a-D_a and O_b-D_b stretching modes, respectively. the latter being at lower frequency because of the intramolecular H-bond $O_a\cdots D_b$ existing in BD monomer.[14] Although the frequency of the O_a-D_a oscillator reported here for BD is close to the value calculated for EG, we observe that the O_b-D_b frequency is at a much lower value than that reported

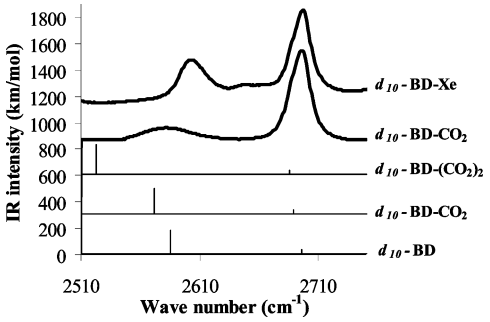

Figure 10. Comparison of the calculated harmonic stretching modes frequencies of BD-d_{10} calculated at the MP2/aug-cc-pVDZ computational level (vertical stick) with the experimental IR spectra.

for EG monomer. This difference is directly related to the strength of the intramolecular hydrogen bond which is higher in BD than in EG. Upon the BD−CO_2 complex formation, we can observe a red shift of 8 cm^{-1} of the O_a-D_a stretching frequency from 2696 to 2688 cm^{-1}, which is directly connected with the LA−LB interaction. Concomitantly, a red shift of 14 cm^{-1} of the O_b-D_b stretching frequency from 2585 to 2571 cm^{-1} is observed which results indirectly from the LA−LB interaction between BD and CO_2. Therefore, in this case, the interaction scheme is different from that found in the EG−CO_2 system. Indeed, the existence of a cooperative H-bond as it exists between CO_2 and EG is no longer possible in the BD−CO_2 system. The intramolecular H-bond existing in BD monomer is so strong and directive toward the O_a atom that it is not directly affected by the presence of CO_2. Actually, it is reinforced indirectly by the LA−LB interaction. Upon the complex formation of BD with a second CO_2 molecule, we can observe that the O_a-D_a stretching frequency is almost unchanged, whereas the O_b-D_b stretching frequency is still redshifted from 2571 to 2522 cm^{-1} because of the LA−LB interaction occurring between BD and the second CO_2 molecule. Therefore, it appears from Figure 10 that the intramolecular H-bond is reinforced by the interaction with the two CO_2 molecules. These calculations explain why we experimentally observe a stronger red shift of the vibration of the O_b-D_b group in the spectra of BD-d_{10} diluted in CO_2 than in xenon, whereas this red shift is only moderate for the O_a-D_a frequency perturbed by a single CO_2 molecule. Although the scaled frequencies reported for BD monomer and BD−CO_2 complexes are not in quantitative agreement with the experimental infrared spectra of BD in scXe and CO_2, respectively, it appears that the general trends observed in the calculated frequency shifts are consistent with the experimental observations. Also, we found it necessary in such double functional molecules to investigate 1:2 complexes to better evaluate the molecular interactions occurring in dense supercritical CO_2.

4.3.3. Charge Distribution. Upon complex formation between the diols and CO_2, a new charge distribution on the two moieties is expected. In particular, major changes should be expected for the atoms directly involved in the diol−CO_2 interactions. Thus, to gain insights into these charge redistributions, we report in Table 3 the changes in the Mulliken atomic charges for the O_a, D_a, O_b, and D_b atoms of EG and BD in the diol−$(CO_2)_2$ complex relative to the monomeric diols. An overall examination put in evidence a systematic gain in electron density on oxygen atoms and a loss in electron density on hydrogen atoms. Also, stronger electron density shifts are observed for O_b-D_b groups compare to O_a-D_a groups.

Concerning EG, it is found that the 1:2 complex formation leads to an increase in the partial positive charge at the hydrogen

TABLE 3: Change in the Natural Population Atomic Charge (Δq, Expressed in *me*) of Diols Atoms under Diol$-(CO_2)_2$ Complexation

species	$\Delta q(O_a)$	$\Delta q(D_a)$	$\Delta q(O_b)$	$\Delta q(D_b)$
1,4-butanediol	−88	62	−94	131
ethylene glycol	−28	20	−36	78

atom D_b by +78 *me* and in the partial negative charge at the oxygen atom O_b by −36 *me*. The binding of the oxygen atom O_a with CO_2 further accentuates the polarization of the whole hydroxyl O_a-D_a group as the partial positive charge at hydrogen increases by +20 *me* and the partial negative charge at oxygen by another −29 *me*. The same trends are observed for BD, but the increase in the partial charges observed for all atoms are more pronounced for BD than for EG. This stronger charge transfer observed for BD is directly related to a larger interaction energy found for BD$-(CO_2)_2$ compared to that calculated for the EG$-(CO_2)_2$ complex.

5. Conclusion

The nature of the interactions between CO_2 and ethylene glycol (EG) or 1,4-butanediol (BD) has been investigated by means of infrared spectroscopic measurements and ab initio calculations. An enhancement of the diols' nucleophilicity is shown upon complex formation with CO_2. This significant reactivity improvement toward electrophilic functions allowed us to synthesize core−shell polyurethane particles without the help of a catalyst. Further investigations are in progress to find out to which extent this relevant promoting effect might be generalized to a larger range of polycondensates.

Acknowledgment. The authors gratefully acknowledge the support provided by the M3PEC computer centre of the DRIMM (Université de Bordeaux I, Talence) for allocating computing time and providing facilities. B.R. acknowledges the Region Aquitaine and CNRS for fellowship.

References and Notes

(1) Jessop, P. G.; Ikaria, T.; Noyori, R. *Science* **1995**, *269*, 1065.

(2) Kendall, J. L.; Canelas, D. A.; Young, J. L.; M., D. J. *Chem. Rev.* **1999**, *99*, 543.

(3) Baiker, A. *Chem. Rev.* **1999**, *99*, 453.

(4) Beckman, E. J. *J. Supercrit. Fluids* **2004**, *28*, 121.

(5) Chambon, P.; Cloutet, E.; Cramail, H. *Macromolecules* **2004**, *37*, 5856.

(6) Chambon, P.; Cloutet, E.; Cramail, H.; Tassaing, T.; Besnard, M. *Polymer* **2005**, *46*, 1057.

(7) Bultinck, P.; Goeminne, A.; Van de Vondel, D. *THEOCHEM* **1995**, *357*, 19.

(8) Frei, H.; Ha, T.-K.; Meyer, R.; Günthard, H. H. *Chem. Phys.* **1977**, *25*, 271.

(9) Gubskaya, A. V.; Kusalik, P. G. *J. Phys. Chem. A* **2004**, *108*, 7151.

(10) Ha, T.-K.; Frei, H.; Meyer, R.; H, G. H. *Theoret. Chim. Acta* **1974**, *34*, 277.

(11) Oie, T.; Topol, I. A.; Burt, S. K. *J. Phys. Chem.* **1994**, *98*, 1121.

(12) Duin, M. V.; Baas, J. M. A.; Graaf, B. V. *J. Org. Chem.* **1986**, *51*, 1298.

(13) Traetteberg, M.; Hedberg, K. *J. Am. Chem. Soc.* **1994**, *116*, 1382.

(14) Lopes Jesus, A. J.; Rosado, M. T. S.; Leitao, M. L. P.; Redinha, J. S. *J. Phys. Chem. A* **2003**, *107*, 3891.

(15) Meredith, J. C.; Johnston, K. P.; Seminario, J. M.; Kazarian, S. G.; Eckert, C. A. *J. Phys. Chem.* **1996**, *100*, 10837.

(16) Poliakoff, M.; Kazarian, S. G.; Howdle, S. M. *Angew. Chem.* **1995**, *34*, 1275.

(17) Lalanne, P.; Tassaing, T.; Danten, Y.; Cansell, F.; Tucker, S. C.; Besnard, M. *J. Phys. Chem. A* **2004**, *108*, 2617.

(18) Fulton, J. L.; Yee, G. G.; Smith, R. D. *J. Am. Chem. Soc.* **1991**, *113*, 8327.

(19) Fulton, J. L.; Yee, G. G.; Smith, R. D. hydrogen bonding in simple alcohols in supercritical fluids: An FTIR study. In *Supercritical Fluid Engineering Science: Fundamental and Applications*; Kiran, E., Brennecke, J. F., Eds.; ACS Symposium Series 514; American Chemical Society: Washington, DC, 1993;, pp 175.

(20) Tassaing, T.; Lalanne, P.; Rey, S.; Cansell, F.; Besnard, M. *Ind. Eng. Chem. Res.* **2000**, *39*, 4470.

(21) Kazarian, S. G.; M. F. Vincent; F. V. Bright; Liotta, C. L.; Eckert, C. A. *J. Am. Chem. Soc.* **1996**, *118*, 1729.

(22) Nelson, M. R.; Borkman, R. F. *J. Phys. Chem. A* **1998**, *102*, 7860.

(23) Raveendran, P.; Wallen, S. L. *J. Am. Chem. Soc.* **2002**, *124*, 12590.

(24) Raveendran, P.; Ikushima, Y.; Wallen, S. L. *Acc. Chem. Res.* **2005**, *38*, 478.

(25) Jamroz, M. H.; Dobrowolski, J. C.; Bajdor, K.; Borowiak, M. A. *J. Mol. Struct.* **1995**, *349*, 9.

(26) Kollmann, P. *J. Am. Chem. Soc.* **1977**, *99*, 4875.

(27) Morokuma, K. *Acc. Chem. Res.* **1977**, *10*, 294.

(28) Danten, Y.; Tassaing, T.; Besnard, M. *J. Phys. Chem. A* **2002**, *106*, 11831.

(29) Saharay, M.; Balasubramanian, S. *J. Phys. Chem. B* **2006**, *110*, 3782.

(30) Frisch, M. J.; Trucks, G. W.; Schlegel, H. B.; Scuseria, G. E.; Robb, M. A.; Cheeseman, J. R.; Montgomery, J. A., Jr.; T. V.; Kudin, K. N.; Burant, J. C.; Millam, J. M.; Iyengar, S. S.; Tomasi, J.; Barone, V.; Mennucci, B.; Cossi, M.; Scalmani, G.; Rega, N.; Petersson, G. A.; Nakatsuji, H.; Hada, M.; Ehara, M.; Toyota, K.; Fukuda, R.; Hasegawa, J.; Ishida, M.; Nakajima, T.; Honda, Y.; Kitao, O.; Nakai, H.; Klene, M.; Li, X.; Knox, J. E.; Hratchian, H. P.; Cross, J. B.; Bakken, V.; Adamo, C.; Jaramillo, J.; Gomperts, R.; Stratmann, R. E.; Yazyev, O.; Austin, A. J.; Cammi, R.; Pomelli, C.; Ochterski, J. W.; Ayala, P. Y.; Morokuma, K.; Voth, G. A.; Salvador, P.; Dannenberg, J. J.; Zakrzewski, V. G.; Dapprich, S.; Daniels, A. D.; Strain, M. C.; Farkas, O.; Malick, D. K.; Rabuck, A. D.; Raghavachari, K.; Foresman, J. B.; Ortiz, J. V.; Cui, Q.; Baboul, A. G.; Clifford, S.; Cioslowski, J.; Stefanov, B. B.; Liu, G.; Liashenko, A.; Piskorz, P.; Komaromi, I.; Martin, R. L.; Fox, D. J.; Keith, T.; Al-Laham, M. A.; Peng, C. Y.; Nanayakkara, A.; Challacombe, M.; Gill, P. M. W.; Johnson, B.; Chen, W.; Wong, M. W.; Gonzalez, C.; Pople, J. A. *Gaussian 03*, Revision C.02 ed.; Gaussian: Wallingford, CT, 2004.

(31) Moller, C.; Plesset, M. S. *Phys. Rev.* **1934**, *46*, 618.

(32) Dunning, T. H. *J. Chem. Phys.* **1989**, *90*, 551.

(33) Wilson, A. K.; Mourik, T. V.; Dunning, T. H. *J. Mol. Struct.* **1996**, *388*, 339.

(34) Tatewaki, H.; Huzinaga, S. *J. Comput. Chem.* **1980**, *3*, 205.

(35) Kendall, R. A.; Dunning, T. H.; Harrison, R. J. *J. Chem. Phys.* **1992**, *96*, 6796.

(36) Murcko, M. A.; DiPaola, R. A. *J. Am. Chem. Soc.* **1990**, 10010.

(37) Boys, S. F.; Bernardi, F. *Mol. Phys* **1970**, *19*, 553.

(38) Danten, Y.; Tassaing, T.; Besnard, M. *J. Phys. Chem. A* **2005**, *109*, 3250.

(39) Mierzwicki, K.; Latajka, Z. *Chem. Phys. Lett.* **2003**, *380*, 654.

(40) Wilson, E. B.; Decius, J. C.; Cross, P. C. *Molecular Vibrations*; McGraw-Hill: New York, 1955.

(41) Scott, A. P.; Radom, L. *J. Phys. Chem.* **1996**, *100*, 16502.

(42) Irikura, K. K.; Johnson, R. D.; Kacker, R. N. *J. Phys. Chem. A* **2005**, *109*, 8430.

(43) Schaftenaar, G.; Noordik, J. H. *J. Comput.-Aided Mol. Des.* **2000**, *14*, 123.

(44) Bowman, L. E.; Palmer, B. J.; Garett, B. C.; Fulton, J. L.; Yonker, C. R.; Pfund, D. M.; Wallen, S. L. *J. Phys. Chem.* **1996**, *100*, 18327.

(45) Tassaing, T.; Oparin, R.; Danten, Y.; Besnard, M. *J. Supercrit. Fluids* **2005**, *33*, 85.

(46) Howard, D. L.; Jorgensen, P.; Kjaergaard, H. G. *J. Am. Chem. Soc.* **2005**, *127*, 17096.

(47) Fraser, G. T.; Pine, A. S.; Suenram, R. D.; Dayton, D. C.; Miller, R. E. *J. Chem. Phys.* **1989**, *90*, 1330.

(48) Block, P. A.; Marshall, M. D.; Pederdsen, L. G.; Miller, R. E. *J. Chem. Phys.* **1992**, *96*, 7321.

(49) Gu, Y.; Kar, T.; Scheiner, S. *J. Am. Chem. Soc.* **1999**, *121*, 9411.